PROCEEDINGS of the
23rd International Congress on Acoustics
9 to 13 September 2019 in Aachen, Germany

Prediction of Acoustic Emission of a Rigid Electrodes DEAP Loudspeaker

Emiliano RUSTIGHI[(1)], William KAAL[(2)], Sven HEROLD[(2)], Łukasz JANKOWSKI[(3)]

[(1)]University of Southampton, United Kingdom, er@isvr.soton.ac.uk

[(2)]Fraunhofer-Institut für Betriebsfestigkeit und Systemzuverlässigkeit LBF, Germany, william.kaal@lbf.fraunhofer.de and sven.herold@lbf.fraunhofer.de

[(3)]Institute of Fundamental Technological Research (IPPT PAN), Poland, ljank@ippt.pan.pl

Abstract

Dielectric Electro-Active Polymers (DEAPs) are lightweight materials whose dimensions change significantly when subjected to electric stimulation. One form of DEAP construction consists of a thin layer of dielectric sandwiched between two perforated rigid electrodes. They can be used as an actuator or a sensor and have the potential to be an effective replacement for many conventional transducers. This paper refers to their use as loudspeakers. To date, flat DEAP loudspeakers have been prototyped and tested but no numerical prediction of their acoustic performance has been presented. In this paper an elemental model is presented. The electro-dynamic behaviour of the electrodes and dielectric layers is taken into account. The acoustic impedance is calculated assuming baffled conditions. The impedances of the individual layers are stacked together and preliminary results are shown.

Keywords: Loudspeaker, DEAP, Sound power

1 INTRODUCTION

Dielectric Electric Active Polymers (DEAP) actuators are a new type of actuators characterised by large strokes, low weight and low cost. They have been used in different applications among which robotics, haptics, energy harvesting, vibration control, sensing and acoustics [1]. In their classical configuration, an elastomer is sandwiched between two compliant electrodes and their working principle is based on compliant electrodes: when voltage is supplied to the electrodes, an electromechanical pressure squeezes the composite structure [2]. Because of the electromechanical pressure, both axial and transversal deformations are experienced. To obtain a useful stroke and force range for actuation purposes, several configurations are used, which may involve mechanical bias (e.g., an external pressure, deformable frames or internal springs) or stacking and folding approaches.

A novel design for such actuators has been recently proposed which utilises rigid-perforated metal electrodes [3]. This design shows a more homogeneous strain distribution, highly conductive electrodes and a high breakdown voltage across a large range of deformations. It proves to be especially advantageous for applications where only moderate strains are needed, but good dynamics and load-bearing capabilities are required. In contrast to conventional designs, such actuators only contract in one direction, whereas all other directions remain undeformed. In this way, it is possible to build actuators made of few layers only, which are of particular interest to realise extremely flat loudspeakers.

Dielectric elastomer loudspeakers with compliant electrodes have been proposed in different configurations [1, 4]. In a similar way to electrostatic loudspeakers, a thin dielectric film radiates sound in response to an oscillating voltage. Their operation voltage is of the order of 1 kV and characterised by a bias and a modulation component. While the bias voltage applies an electromechanical pre-straining which is beneficial to the overall performances, the modulation component of the voltage is responsible for the sound generation. Compared to traditional loudspeakers they have a smaller mechanical impedance and are able to achieve larger displacements. Hence, a high sound pressure field can be generated with loudspeakers of moderate size. Because of their deformation mechanisms, they are in some ways analogous to monopole sources and they can potentially

show better directivity performance than traditional loudspeakers. However, since the displacement is driven by Maxwell pressure law [2], they are inherently nonlinear.

A prototype of a flat DEAP loudspeaker with perforated rigid electrodes has been previously built and tested [5]. In relation to compliant electrode loudspeakers, such design does not need mechanical bias and the increased conductivity of the rigid electrodes allows for the use of less demanding amplifiers and to cover the full audible frequency range. Such novel loudspeakers are lighter, cheaper and thinner than conventional loudspeakers. In fact, differently from conventional coil loudspeakers, no resonating sound box is needed and an extremely flat configuration can be obtained. In addition, since they do not need a mechanical bias, the sound emitting film can be manufactured in any desired shape. To date no model is available to predict the acoustic performance of a rigid electrodes DEAP loudspeaker. In this paper an elemental model is presented, where the electrodes are modelled as bending plates, the dielectric as a Winkler bedding and the acoustic impedance calculated assuming baffled conditions.

2 MECHANICAL MODEL OF THE ELECTRODES

The electrodes are assumed as extensionally rigid but compliant in bending. Hence, the electrodes are modeled as uniform thin circular plates of radius a with free boundary conditions and made of homogeneous and isotropic material. The appropriate boundary condition is then applied once they are combined with the dielectric layers. The analytical expressions of the natural frequencies f_{mn} and mode shapes ϕ_{mn} given in [6] have been used to calculate the mobility matrix of each electrode by modal summation.

In order to do so the plate is discretised in element of equal area, ΔS, following the model suggested by Arenas [7]. In order to discretise the disc in elements of the same area, the radius is firstly divided into N equally spaced elements. Each concentric rings then in divided in a series of areas multiple of the previous. In this paper, the central area has been divided arbitrarily in four elements so to get $4N^2$ elements in total. Hence the area of each element will be

$$\Delta S = \frac{\pi}{4}\left(\frac{a}{N}\right)^2 \tag{1}$$

Figure 1 shows the elemental discretisation used in this paper ($N = 8$) and an example of calculated point mobility at the centre of one of the elements. The properties of the disc are given in Table 1.

The perforation of the electrodes affects both density and bending stiffness of the electrodes. It has been assumed that the perforation has no effect on the effective Poisson ratio of the electrodes. The perforation considered in this paper is a regular triangular pattern as shown in figure 2. The ligament efficiency is the non-dimensional parameter used to characterise the perforation density

$$l_\mathrm{e} = \frac{d}{p} \tag{2}$$

where p is the pitch of the pattern and $d = p - 2R$ where R is the radius of the perforation holes. Such parameter conveniently span between 1 (no perforation) and 0 (maximum perforation) the full range of possible perforation's densities.

The effective density of the perforated plate ρ_e is considered to be reduced by the perforation using a mixing law as:

$$\rho_e = \rho(1 - \phi_A) \tag{3}$$

where ϕ_A is the open area ratio, which, for circular perforations, is related to the ligament efficiency by $\phi_A = \frac{\pi}{2\sqrt{3}}(1 - l_\mathrm{e})^2$. The effect the perforation has on the bending stiffness has been taken into account using the simplified formula proposed by Soler and Hill [8]:

$$D_e = D(1 - \phi_A)_e^\lambda \tag{4}$$

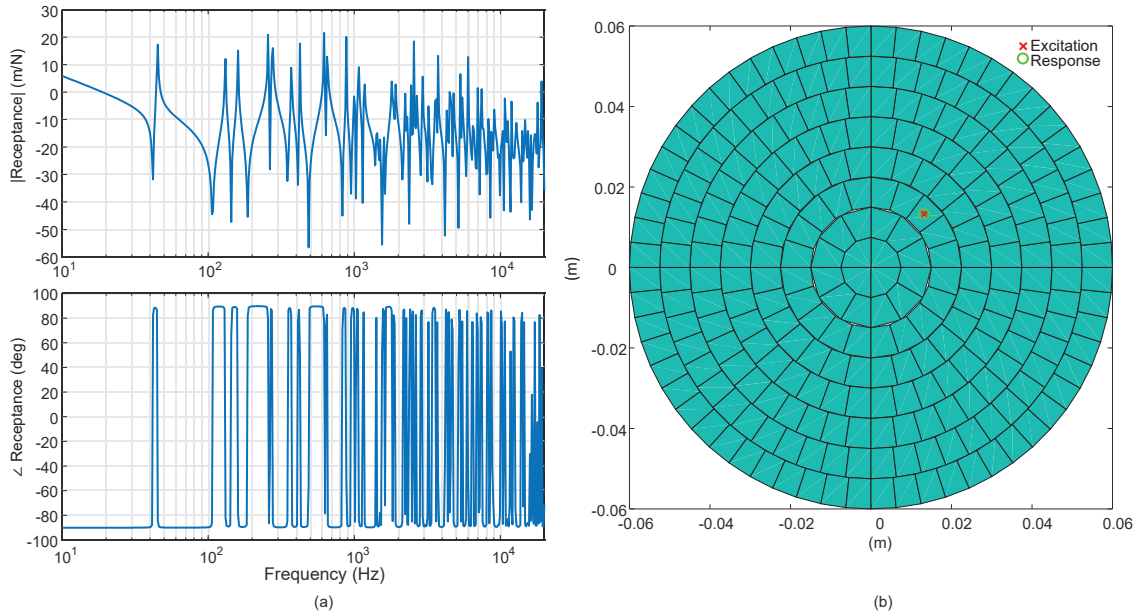

Figure 1. Point mobility (a) for a freely suspended disc computed at the centre of the marked area (b).

where D is the bending stiffness of the non-perforated plate and the parameter λ_e is obtained as

$$\lambda_e = \frac{13+3\phi}{8}\left[1+\frac{3-\phi}{4}\frac{d}{p}+\frac{1+\phi}{2}\frac{d}{p}\left(1-\frac{d}{p}\right)^2\right] \tag{5}$$

with

$$\phi = \frac{\frac{h}{2p}-1}{\frac{h}{2p}+1}. \tag{6}$$

3 ELECTRO-MECHANICAL MODEL OF THE SOFT DIELECTRIC LAYER

3.1 Effective mechanical stiffness

The dielectric layers have been simply modelled as a Winkler bedding, i.e. as a set of parallel independent impedances each of them representing the material underneath the discretised area ΔS. No viscoelastic behaviour is assumed here. The equilibrium of one element can be obtained using the Neo-Hookean hyperelastic material expression for natural rubber in compression [9]:

$$\left(\lambda-\frac{1}{\lambda^2}\right)\frac{Y_d}{3}+p_M = f(t) \tag{7}$$

where λ is the stretch ratio and Y_d is the effective dielectric Young's modulus. Because of the perforation in the electrodes the dielectric material (natural rubber) will tend to bulge into the holes. The macroscopic result of this is a reduction of the effective Young's modulus of a factor ψ_A, i.e. $Y_d = \psi_A Y$, with Y the nominal dielectric Young's modulus. Such factor has been estimated numerically by a FEM analysis using an equivalent axial-symmetric model of an individual cell. The results obtained have been summarised in Figure 3 where also the influence of the thickness of the dielectric layer is included. In the previous equation, $f(t)$ is an applied external force which is zero in this application and p_M is the Maxwell pressure, which is the same as that of a

parallel plate rigid capacitor since there is no change in the area during deformation [1]:

$$p_M = \frac{\varepsilon_0 \varepsilon}{2} \left(\frac{V(t)}{z} \right)^2 \tag{8}$$

where ε is the relative dielectric constant of the polymer, ε_0 is the dielectric constant of free space, V is the applied voltage and z is the film thickness. When no external force is applied, the effect of the applied voltage is to squeeze the dielectric layer. It is then possible to compute the equilibrium thickness $\bar{z}$ to an applied constant voltage as:

$$\bar{z} = \sqrt[3]{z_0^3 - \frac{3\varepsilon\varepsilon_0 z_0}{2Y_d} V^2} \tag{9}$$

If a small external pressure is applied to the element we can linearise around the equilibrium position to obtain the effective mechanical stiffness as a function of V.

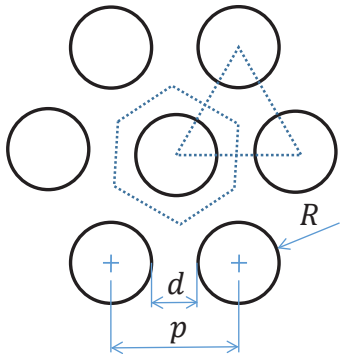

Figure 2. Perforation geometry: radius of the perforation R, pitch of the pattern p and ligament d.

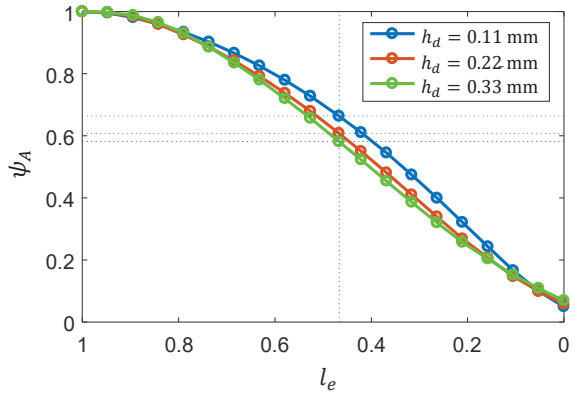

Figure 3. Stiffness correction factor ψ_A due to the perforation of the electrodes compressing the dielectric layer.

3.2 Voltage driven response

When the loudspeaker is driven with a simple harmonic signal of frequency ω and amplitude V_{AC} it is also necessary to offset this signal by a constant V_{DC} in order to avoid the reversing of the actuation. Since the voltage is squared in equation (8), the alternate voltage has the effect of changing the stiffness but at the same time creates parametric stiffness terms. The two parametric stiffnesses have been here neglected since much smaller than the non-parametric terms. In this case the loudspeaker driven excitation f_V is composed of two frequencies at the fundamental frequency ω and at twice the excitation frequency 2ω:

$$f_V = -(1-\psi_A)\Delta S \frac{\varepsilon\varepsilon_0}{2\bar{z}^2} \left(V_1^2 \mathrm{e}^{\mathrm{i}\omega t} + V_2^2 \mathrm{e}^{\mathrm{i}2\omega t} \right) \tag{10}$$

where $V_1 = 2V_{\mathrm{DC}}V_{\mathrm{AC}}$ and $V_2 = V_{\mathrm{AC}}^2/2$.

4 CALCULATION OF ACOUSTIC EMISSIONS

4.1 Mobility assembling approach

In order to assemble the impedance matrices of each layer a procedure similar to the frequency based sub-structuring [10, 11] has been adopted. The methodology had however to be adapted to this particular case. In

fact, since a free-free structure includes rigid body motions, its impedance or mobility matrix is singular and rank deficient, and hence the inverse of the stiffness does not exist. For this reasons care must be taken into assembling the substructures.

The first step is to assemble the first electrode to a grounded dielectric, as illustrated in Figure 4 . The assembled mobility matrix $\mathbf{Y}_{GE}$ is obtained applying compatibility and equilibrium conditions, and it expressed as

$$\mathbf{Y}_{GE} = \mathbf{Y}_E \left(\mathbf{I} + \mathbf{Z}_G \mathbf{Y}_E\right)^{-1} \tag{11}$$

where $\mathbf{I}$ is the identity matrix, $\mathbf{Z}_G$ is the grounded dielectric impedance matrix and $\mathbf{Y}_E$ is the electrode mobility matrix, which are given respectively by:

$$\mathbf{Z}_G = \frac{-\mathrm{i}k_{\mathrm{ru,el}}}{\omega}\mathbf{I} \tag{12}$$

$$\mathbf{Y}_E = \mathbf{B}\mathrm{diag}\left(\frac{1}{M_{mn}}\frac{\mathrm{i}\omega}{\omega_{mn}^2(1+\mathrm{i}\eta_{mn})-\omega^2}\right)\mathbf{B}^{\mathrm{T}} \tag{13}$$

where M_{mn}, ω_{mn}, η_{mn} and $\mathbf{B}$ are the modal masses, natural frequencies, modal loss factors and modal matrix of the electrode.

Once the mobility of the first dielectric electrode is obtained it is possible to assemble the next dielectric layer where the internal dofs can be neglected in order to keep low the size of the final mobility matrix. Figure 5 gives an illustration of the process. The final assembled mobility matrix is given by

$$\mathbf{Y} = \left[\mathbf{Z}_{FF} - \mathbf{Z}_{FI}\left(\mathbf{I} + \mathbf{Y}_{GE}\mathbf{Z}_{II}\right)^{-1}\mathbf{Y}_{GE}\mathbf{Z}_{IF}\right]^{-1} \tag{14}$$

where the impedances matrices $\mathbf{Z}_{ij}$ are sub-matrices of the full impedance matrix of the dielectric layer as indicated in the following equation

$$\begin{Bmatrix}\mathbf{f}_R^F \\ \mathbf{f}_R^I\end{Bmatrix} = \begin{bmatrix}\mathbf{Z}_{FF} & \mathbf{Z}_{FI} \\ \mathbf{Z}_{IF} & \mathbf{Z}_{II}\end{bmatrix}\begin{Bmatrix}\mathbf{v}_R^F \\ \mathbf{v}_R^I\end{Bmatrix} \tag{15}$$

Then again Equation 11 and Equation 14 can be used again for adding as many layers as requested.

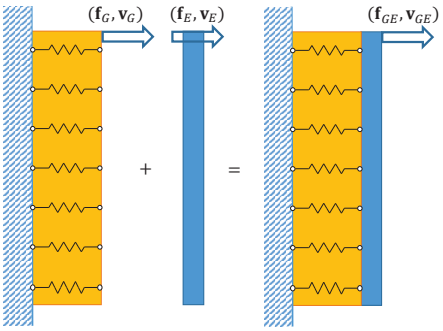

Figure 4. Assembling the electrode to a grounded layer.

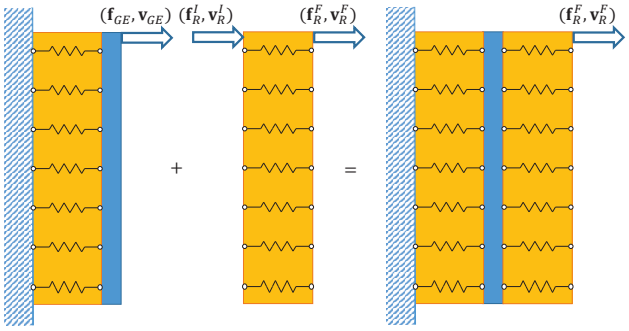

Figure 5. Assembling a dielectric layer to a grounded actuator.

4.2 Emitted Sound Power

By definition the radiated sound power W is

$$W = \frac{\Delta S}{2}\mathbb{R}\mathrm{e}\left[\mathbf{v}^{\mathrm{H}}\mathbf{Z}_A\mathbf{v}\right] \tag{16}$$

where H is the complex conjugate transpose or Hermitian operator and $\mathbf{Z}_A$ is the *specific acoustic impedance* matrix. Assuming that each element can be approximated to a circular pistonic radiator the specific acoustic impedance matrix can be expressed as in [12]:

$$\mathbf{Z}_A = \begin{bmatrix} \rho c \left[1 - \frac{J_1(2ka_i)}{ka_i} + \mathrm{i}\frac{S_1(2ka_i)}{ka_i}\right] & \frac{\rho c k^2 \Delta S}{2\pi}\left[2\frac{J_1(ka_i)}{ka_i}\right]^2\left[\frac{\sin(kd_{21})}{kd_{21}} + \mathrm{i}\frac{\cos(kd_{21})}{kd_{21}}\right] & \cdots \\ \frac{\rho c k^2 \Delta S}{2\pi}\left[2\frac{J_1(ka_i)}{ka_i}\right]^2\left[\frac{\sin(kd_{21})}{kd_{21}} + \mathrm{i}\frac{\cos(kd_{21})}{kd_{21}}\right] & \rho c \left[1 - \frac{J_1(2ka_i)}{ka_i} + \mathrm{i}\frac{S_1(2ka_i)}{ka_i}\right] & \\ \vdots & & \ddots \end{bmatrix} \tag{17}$$

where ρ is the air density, c is the sound speed in air, $k = \frac{\omega}{c}$ is the wave number of sound, J_1 is the first-order Bessel function, S_1 is the Struve function and i is the imaginary unit, d_{ij} is the distance between the centers of two circular elements, respectively. Also the the radiation efficiency, defined as ratio of the radiated sound power over the mean radiation, and the kinetic energy of the top electrode can be easily computed.

5 SOME COMPUTATIONAL RESULTS

5.1 A loudspeaker prototype

A loudspeaker prototype was previously realised using largely available materials (see Figure 6). The electrodes were made from 0.5 mm thick perforated mild steel sheets with 0.8 mm diameter holes and 1.5 mm pitch. The dielectric material used was 0.11 mm thick latex exercise bands (Tan Extra-Thin Thera Band®). The electrode diameters was 120 mm. The electrodes have two wings for powering which have been curved. This design aims to lower their bending stiffness so that restrictions to vibration of the electrode is kept to a minimum. The properties of such prototype are reported in Table 1 and will be used for the following calculations. A measurement of the radiated sound power, as shown in Figure 7(a), was performed in a resonant box applying a pseudo-random noise with a peak-to-peak voltage of about 80 V and an offset voltage of 800 V. Two, four and ten layers loudspeakers were considered. It is noteworthy that the high response below 300 Hz was due to background noise. It is also surprising that the high response at 500 Hz is not affected by the number of layers.

Table 1. Calculations parameters.

	Description	Value		Description	Value
a	Radius of the loudspeaker	0.06 m	η_e	Loss factor of electrodes	0.001
V_{DC}	Supply voltage offset	1000 V		Total number of elements	256
ρ_e	Density of electrodes	5800 kgm^{-3}	V_{AC}	Alternate supply voltage	200 V
h_e	Thickness of electrodes	0.5 mm	ε	Relative dielectric constant	0.001
p	Pitch of perforation	1.5 mm	h_d	Thickness of dielectric	0.11 mm
R	Radius of perforation holes	0.4 mm	E_d	Young's mod. of dielectric	5 MPa
l_e	Ligament efficiency	0.47	ν_d	Poisson ratio of dielectric	0.45
E_e	Young's mod. of electrodes	210e9 Pa	η_d	Loss factor of dielectric	0.05
ν_e	Poisson ratio of electrodes	0.33	Ψ_A	Perforation factor	0.6639

5.2 Preliminary results

The sound radiation power has been computed for the loudspeaker shown in Figure 6. Figure 7(b) shows the predicted sound radiation power for 2, 4 and 10 layers. It has been assumed that only an alternate voltage of 80 V contributes to the loudspeaker excitation. The response at low frequency in the experimental results is mainly due to background noise. The model shows instead a slope of 40dB per decade. This reflects a monopole radiation mode driven by a constant force over the frequency. In fact, both the monopole radiation

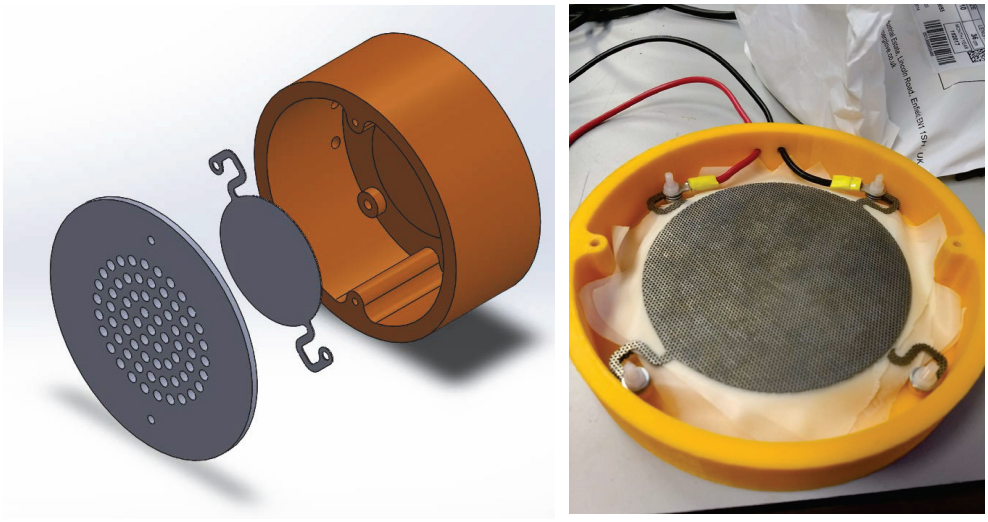

(a) (b)

Figure 6. Design of a DEAP loudspeaker (a) and its realisation (b).

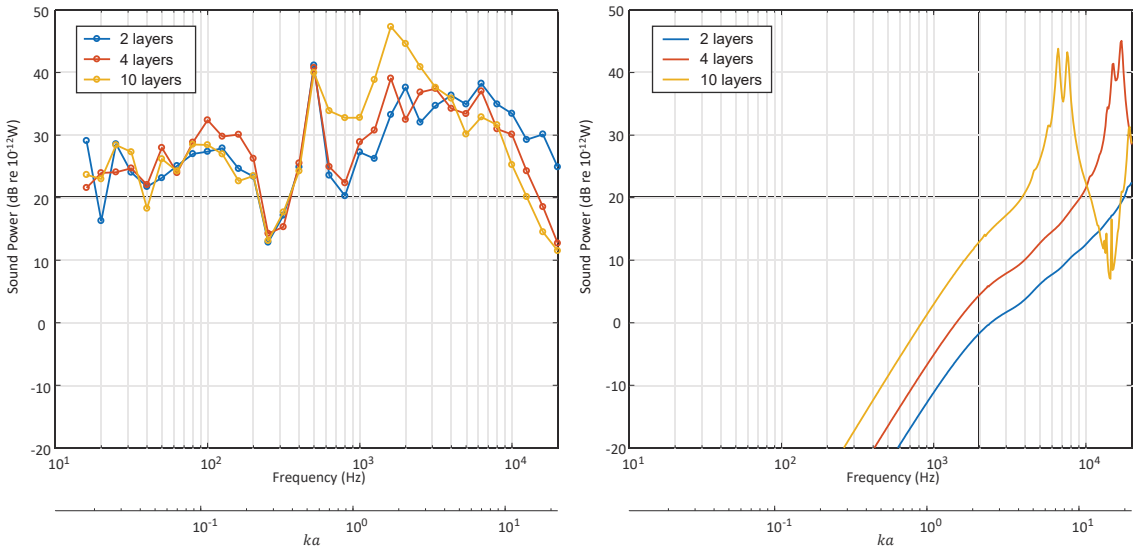

Figure 7. Predicted sound radiation powers for DEAP loudspeakers of 2, 4 and 10 layers: electrodes assumed as rigid bodies (a) or flexible plates (b). (k is the acoustic wavenumber)

and the mobility of the structure grow at 20dB per decade. From these preliminary results it can be seen the model is able to roughly predict the radiated sound power levels at higher frequencies. However, the resonant peaks are not accurate and it seems that the model is far more stiff than the actual prototype. This is probably caused by the imperfect planarity of the electrodes which reduces the contact area between dielectrics and electrodes. Also the effect of increasing the number of layers is more apparent in the simulated results and at

very high frequencies the experimental sound power decreases more for a larger number of layers. This is due to the amplifier limited power in driving higher capacitive loads.

6 CONCLUSIONS

In this paper a new approach to model the acoustic emissions of a stacked DEAP loudspeaker with perforated electrodes has been proposed. Preliminary numerical results have been compared with experimental data showing that the model is able to reproduce the physics of the real system. However, material properties needs to be tuned in order to improve the match at resonances.

ACKNOWLEDGEMENTS

This project has been supported by the Royal Society International Exchanges scheme.

REFERENCES

[1] Carpi F, De Rossi D, Kornbluh R, Pelrine RE, Sommer-Larsen P. Dielectric elastomers as electromechanical transducers: Fundamentals, materials, devices, models and applications of an emerging electroactive polymer technology. Elsevier; 2011.

[2] Pelrine RE, Kornbluh RD, Joseph JP. Electrostriction of polymer dielectrics with compliant electrodes as a means of actuation. Sensors and Actuators A: Physical. 1998;64(1):77–85.

[3] Kaal W, Herold S. Numerical investigations on dielectric stack actuators with perforated electrodes. Smart Materials and Structures. 2013;22(10):104016.

[4] Heydt R, Kornbluh R, Eckerle J, Pelrine R. Sound radiation properties of dielectric elastomer electroactive polymer loudspeakers. In: Smart Structures and Materials 2006: Electroactive Polymer Actuators and Devices (EAPAD). vol. 6168. International Society for Optics and Photonics; 2006. p. 61681M.

[5] Rustighi E, Kaal W, Herold S, Kubbara A. Experimental Characterisation of a Flat Dielectric Elastomer Loudspeaker. Actuators. 2018;7(2). Available from: http://www.mdpi.com/2076-0825/7/2/28.

[6] Amabili M, Pasqualini A, Dalpiaz G. Natural frequencies and modes of free-edge circular plates vibrating in vacuum or in contact with liquid. Journal of sound and vibration. 1995;188(5):685–699.

[7] Arenas JP. Numerical computation of the sound radiation from a planar baffled vibrating surface. Journal of Computational Acoustics. 2008;16(03):321–341.

[8] Soler A, Hill W. Effective bending properties for stress analysis of rectangular tubesheets. Journal of Engineering for Power. 1977;99(3):365–370.

[9] Treloar L. The elasticity and related properties of rubbers. Reports on progress in physics. 1973;36(7):755.

[10] Cuppens K, Sas P, Hermans L. Evaluation of the FRF based substructuring and modal synthesis technique applied to vehicle FE data. In: Proceedings of the International Seminar on Modal Analysis. vol. 3. KU Leuven; 1998; 2001. p. 1143–1150.

[11] de Klerk D, Rixen DJ, de Jong J. The frequency based substructuring (FBS) method reformulated according to the dual domain decomposition method. In: 24th international modal analysis conference. vol. 36. Springer New York; 2006. .

[12] Hashimoto N. Measurement of sound radiation efficiency by the discrete calculation method. Applied Acoustics. 2001;62(4):429–446.